HEART RATE VARIABILITY MEASUREMENT USING THE SECOND DERIVATIVE PHOTOPLETHYSMOGRAM

Mohamed Elgendi, Mirjam Jonkman and Friso DeBoer
School of Enigneering and Information Technology, Charles Darwin University, Australia

Keywords: Heart Rate, HRV, Plethysmography, SDPTG.

Abstract: Heart-rate monitoring is a basic measure for cardiovascular functionality assessment. The electrocardiogram (ECG) and Holter monitoring devices are accurate, but their use in the field is limited. Photoplethysmography is an optical technique that has been developed for experimental use in vascular disease. Because of its non-invasive, safe, and easy-to-use properties, it is considered a promising tool that may replace some of the current traditional cardiovascular diagnostic tools. A useful algorithm for *a*-wave detection in the second derivative plethysmogram (SDPTG) is introduced for heart–rate monitoring. The performance of the proposed method was tested on 27 records measured at rest and after exercise. Statistical HRV measures can be calculated using the *a*-*a* interval of the SDPTG.

1 INTRODUCTION

Heart rate variability has considerable potential to assess autonomic nervous system fluctuations in normal healthy individuals and in patients with various cardiovascular and non-cardiovascular disorders. Heart rate variability (HRV) studies could enhance our understanding of physiological phenomena, the actions of medications, and disease mechanisms.

Traditionally, HRV measures are based on cardiac inter-beat intervals using the electrocardiogram (ECG). Some practitioners, however, have used a distal measurement of the arterial pulse like the fingertip photoplethysmogram to measure the heart rate. However, there are some potential obstacles to obtaining precise inter-beat intervals from arterial pressure pulses, especially when measured from a distal source like fingertip photoplethysmogram. The lack of sharp peaks in blood pressure pulses compared to the R-peaks in the ECG makes the accurate determination of heart rate challenging. Also the shape and timing of the pulse waveform may be influenced by ventricular pressure, flow rate, time period, or other parameters of cardiac output. Peripheral effects, such as changes in vascular tone, may also influence distal pulse peak detection.

(Berntson et al., 1997) reported these potential drawbacks of the fingertip plethysomograph. Therefore, they strongly advised the usage of R-R intervals from ECG signals to determine interbeat intervals. However, they also stated that "the use of intra-arterial pressure pulses and a sophisticated peak detection algorithm may be acceptable," and also recommended, Their opinion is that indirect measures, such as photoplethymographic signals require further validation.

(Giardino et al., 2002) proved that distal pulse pressure is adequate for determining the heart rate variability under resting conditions. Their results provided grounds for some caution in the use of finger plethysmography in experimental studies, where manipulations may alter the relationship between cardiac chronotropic control and distal blood pressure changes in unpredictable ways. They recommended further studies that include test–retest reliability assessment of different data collection techniques.

The the second derivative of photoplethysmogram (SDPTG) was developed as a method to allow more accurate recognition of the inflection points and easier interpretation of the original plethysmogram wave.

In literature, the second derivative of photoplethysmogram (SDPTG) has also been called acceleration plethysmogram (APG). In this paper, the abbreviation SDPTG will be used.

Elgendi M., Jonkman M. and DeBoer F. (2010).
HEART RATE VARIABILITY MEASUREMENT USING THE SECOND DERIVATIVE PHOTOPLETHYSMOGRAM.
In *Proceedings of the Third International Conference on Bio-inspired Systems and Signal Processing*, pages 82-87
DOI: 10.5220/0002743300820087

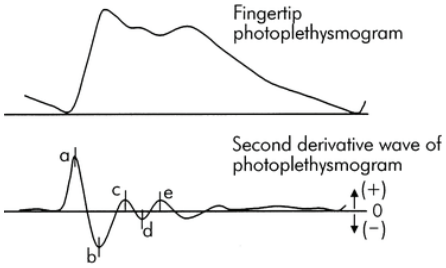

Figure 1: Signal Measurements (a) Original fingertip photoplethysmogram (b) second derivative wave of photoplethysmogram (SDPTG).

As shown in Fig.1, The heart beat in SDPTG consists of four systolic waves and one diastolic waven (Takazawa et al., 1993), namely *a*-wave (early systolic positive wave), *b*-wave (early systolic negative wave), *c*-wave (late systolic reincreasing wave), *d*-wave (late systolic redecreasing wave) and *e*-wave (early diastolic positive wave). The height of each wave was measured from the baseline, with the values above the baseline being positive and those under it negative.

Because the peaks in the SDPTG signal are more clearly defined than in the original photoplethysmographic signal is more suitable for accurate heart rate detection.

(Taniguchi et al., 2007) used *a*-*a* interval in the second derivative photoplethysmogram instead of R-R interval in the ECG to determine the heart rate evaluating stress that surgeons experience.

To calculate the heart rate variability (HRV) using the second derivative photoplethysmogram (SDPTG), the accurate detection of individual *a*-waves is a first essential step.

Although the clinical significance of using SDPTG signals has been discussed, there is still a lack of studies focusing on the automatic detection of *a*-waves in SDPTG signals.

In this paper, we present an algorithm that can be used to calculate the heart rate variability using the finger photoplethysmograph. This investigation aimed to develop a fast and robust algorithm to detect *a*-waves in SDPTG signals. The SDPTG waveform was measured in a population-based sample of healthy males at rest and after exercise.

2 DATA

The photoplethysmograms of twenty seven healthy males volunteers with a mean±SD age of 27±6.9 were measured by a photoplethysmograph (Salus), equipped with a sensor located at the cuticle of the second digit of the left hand. Measurements were performed while the subject was at rest on a chair. Data were collected at a sampling rate of 200Hz. The duration of each data segment is 20 seconds.

The test was conducted from 20th of April to 5th of May 2006 at Northern Territory Institution of Sport (NTIS).

All procedures were approved by the ethics committee of Charles Darwin University. Informed consent was obtained from all volunteers.

3 METHODOLOGY

An algorithm to detect *a*-waves is described below. The algorithm consists of three main stages: pre-processing, feature extractions and thresholding. The structure of the algorithm is shown in Fig. 2.

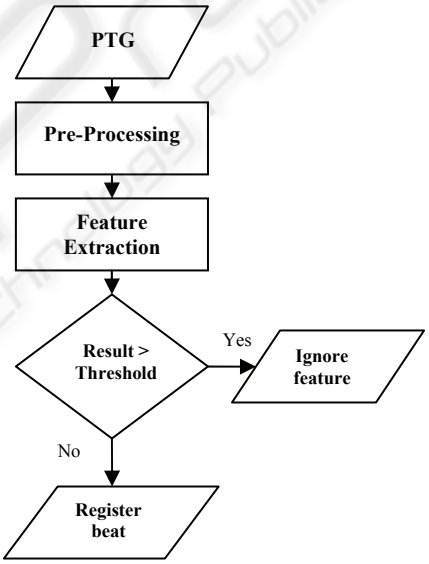

Figure 2: Algorithm structure.

3.1 Pre-Processing

The pre-processing stage consists of two sub-stages: bandpass filtering and taking the second derivative of the photoplethysmogram.

3.1.1 Bandpass Filter

We remove the baseline wander and high frequencies which do not contribute to *a*-waves detection by using a second order Butterworth filter with passband 0.5-10 Hz.

$$s[n] = Butterworth(PTG[n], 0.5-10Hz)$$

Fig. 3(b) is the result of applying a Butterworth filter to the original signal shown in Fig. 3(a)

3.1.2 Second Derivative

z[n] shown in Fig. 3(c) is the second derivative of the filtered photoplethysmogram *s[n]*. Inflection points are seen as peaks in the SDPTG.

3.2 Feature Extraction

The feature extraction stage consists of two sub-stages: squaring and selection of potential blocks.

3.2.1 Squaring

y[n] is the square of the SDPTG signal *z[n]*. Squaring the signal makes the results positive and emphasizes large differences

3.2.2 Selection of Potential Blocks

We demarcate the onset and offset of the potential *a*-waves in the SDPTG signals by using two moving averages, based on the normal duration of the *ab* interval which for a healthy adult is 187±17 ms.

For a sampling frequency of 200 Hz, the maximum window size corresponding to the *ab* interval is approximately 40 points and the maximum window size corresponding to complete heart beat interval is approximately 220 points. We will use the maximum window sizes to detect *a*-waves. The *a*-waves are detected by comparing two moving averages.

First moving-window integration: The fist moving average is., calculated as follows:

$$MA_{Peak}[n] = \frac{1}{W_1}(y[n-(W_1-1)] + y[n-(W_1-2)] + ...+ y[n])$$

Where $W_1 = 40$ which is the window width of *ab* segment. The purpose of the first moving average, shown as the dotted line in Fig. 3(d), is to emphasize the *a*-wave.

Second Moving-window Integration: the second moving average, shown as the solid line in Fig. 3(d), is used as a threshold for the output of the first moving-window integration.

$$MA_{MaxPeak}[n] = \frac{1}{W_2}(y[n-(W_2-1)] + y[n-(W_2-2)] + ...+ y[n])$$

where $W_2 = 220$ is the window width of a complete heart beat.

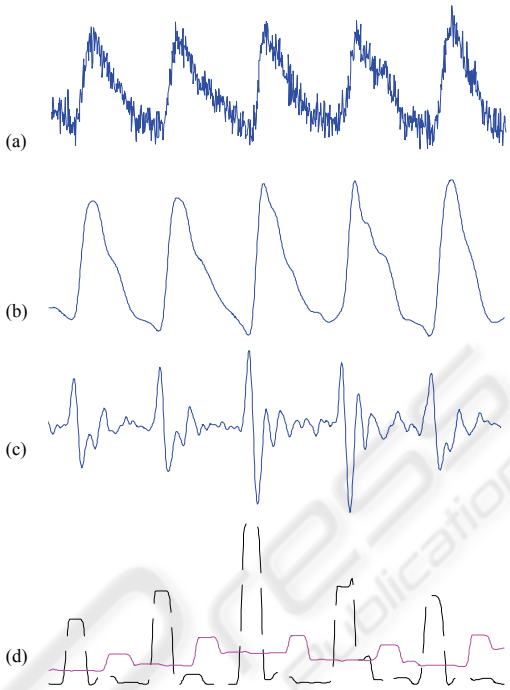

Figure 3: Algorithm structure.(a) original SDPTG signal (b) filtered PTG signal with Butterworth bandpass filter (c) Second Derivative of PTG (d) generating blocks of interest using two moving averages to detect *a*-waves.

When the amplitude of the first moving average filter (MA_{Peak}) is greater than the amplitude of the second moving average filter ($MA_{MaxPeak}$), that part of the signal is selected as a block of interest, as follows:

IF $MA_{Peak}[n] > MA_{MaxPeak}[n]$ **THEN**
$BLOCKS[n] = 1$
ELSE
$BLOCKS[n] = 0$
END

Fig. 3(d) shows an example of applying the two moving averages.

We show four consecutive *aa* intervals in Fig. 3 (d) to demonstrate the idea of using two filters to generate blocks of interest. Sometimes, blocks are generated which do not represent potential *a*-waves. These blocks are caused by noise and need to be eliminated.

3.3 Thresholding

Blocks with a small width are considered as blocks caused by noise. Blocks which are smaller than half of the expected size for the *ab* interval are rejected.

Table 1:*a*-wave detection performance on SDPTG Data.

	Before Exercise				After Exercise 1				After Exercise 2				After Exercise 3			
Record	No of beats	TP	FP	FN	No of beats	TP	FP	FN	No of beats	TP	FP	FN	No of beats	TP	FP	FN
A1	26	26	0	0	45	45	0	0	43	41	2	0	32	32	0	0
A2	24	24	0	0	44	44	0	0	47	47	0	0	46	46	0	0
B1	17	17	0	0	36	36	0	0	44	43	1	0	32	32	0	0
B2	26	26	0	0	43	43	0	0	38	38	0	0	30	30	0	0
C2	20	20	0	0	33	33	0	0	37	37	0	0	40	40	0	0
C3	20	20	0	0	30	30	0	0	23	23	0	0	Could not continue			
D2	22	22	0	0	33	33	0	0	39	39	0	0	42	42	0	0
D3	19	19	0	0	23	23	0	0	27	27	0	0	30	30	0	0
E1	22	22	0	0	25	25	0	0	30	30	0	0	31	31	0	0
E2	22	22	0	0	25	25	0	0	30	30	0	0	31	31	0	0
E3	19	19	0	0	34	34	0	0	38	38	0	0	39	38	1	0
G2	30	30	0	0	48	48	0	0	48	48	0	0	49	49	0	0
G3	19	19	0	0	33	33	0	0	42	42	0	0	45	45	0	0
H3	23	23	0	0	31	31	0	0	32	32	0	0	32	32	0	0
I1	22	22	0	0	30	30	0	0	35	35	0	0	41	41	0	0
I2	17	17	0	0	28	28	0	0	31	31	0	0	31	31	0	0
J2	23	23	0	0	36	36	0	0	41	41	0	0	38	38	0	0
L2	24	24	0	0	36	36	0	0	37	37	0	0	30	30	0	0
L3	24	24	0	0	35	35	0	0	39	39	0	0	41	41	0	0
N2	18	18	0	0	23	23	0	0	24	24	0	0	33	33	0	0
N3	20	20	0	0	29	29	0	0	31	31	0	0	37	37	0	0
O1	24	24	0	0	29	29	0	0	33	33	0	0	38	38	0	0
O2	17	17	0	0	32	32	0	0	34	34	0	0	40	40	0	0
P1	26	26	0	0	35	35	0	0	34	34	0	0	36	36	0	0
P2	20	20	0	0	29	29	0	0	34	34	0	0	39	38	1	0
Q1	22	22	0	0	27	27	0	0	28	28	0	0	29	29	0	0
Q2	18	18	0	0	33	33	0	0	36	36	0	0	34	34	0	0
27 volunteers	584	584	0	0	885	885	0	0	955	952	3	0	946	944	2	0

The expected size for the *ab* interval is based on the statistics for healthy adults, as described above.

We reject blocks that are smaller than 50% of the width that is expected for the *ab* interval. This corresponds to:

$$width(BLOCKS) < 20$$

The rejected blocks are considered as noisy blocks and the accepted blocks are considered to be containing *a*-wave.

The maximum absolute value within each accepted block is considered to be the *a* peak. For this research the algorithm was tested using annotated *a* peaks.

The proposed algorithm was tested on 27 SDPTG records. The volunteers exercised three times. The photoplethysmogram was recorded before starting exercise and after each exercise period. Volunteer C3 discontinued in the third exercise period. No episodes have been excluded from our analysis

The exercise SDPTG data contains records of normal SDPTG signals as well as records of SDPTG signals that are affected by non-stationary effects, low signal-to-noise ratio, and high heart rate. This provides the opportunity to test the robustness of the algorithm in detecting *a*-waves in SDPTG signals. *a*-wave detection may be affected by the quality of the SDPTG recordings and the irrigular heart rhythms in the SDPTG signals.

The following statistical parameters were used to evaluate the algorithm:

$$Se = \frac{\mathrm{TP}}{\mathrm{TP}+\mathrm{FN}}$$

$$+P = \frac{\mathrm{TP}}{\mathrm{TP}+\mathrm{FP}}$$

True Positive (TP): *a*-wave has been classified as *a*-wave.
False Negative (FN): *a*-wave has been missed.
False Positive (FP): Non *a*-wave classified as *a*-wave.

The sensitivity *Se* is the percentage of true *a*-waves that were correctly detected by the algorithm. The positive predictivity *+P* is the percentage of detected *a*-waves which are real *a*-waves.

Table I shows the result of *a*-waves detection in 27 different records of collected SDPTG before exercise and after each of the three exercise periods, containing a total of 3332 heart beats.

As shown in Table 1, records which have relatively irregular fast heart beats signals like A1-after exercise 2 , irregular fast heart beats with low amplitudes like B1-after exercise 2, and non-stationary SDPTG with irregular fast heart beats and low amplitudes like E3-after exercise 3 contain a few false positives (FP).

The number of false negatives (FN) was zero. The overall average sensitivity for *a*-waves detection was 100% and the positive predictivity was 99.88%.

4 DISCUSSION

The major reason for the interest in measuring heart rate variability stems from its ability to predict survival after a heart attack. In ECG signals analysis, the interval between adjacent QRS complexes is termed as the normal to normal (NN) or the R to R (RR) interval. Heart rate variability (HRV) refers to the beat-to-beat alterations in heart rate. The results of a HRV analysis portray the physiological condition of the patient and are an important indicator of cardiac disease. Many studies have shown that reduced HRV predicts sudden death in patients.

The detection of R peak is the main step to measure HRV. Precise R-R interval calculations are necessary to accurately depict the physiological state. (John, 2000) found that more than 26 different types of arithmetic manipulations of R-R intervals have been described in the literature to represent HRV.

The Task Force of the European Society of Cardiology and the North American Society of Pacing and Electrophysiology (Task Force of the European Society of Cardiology and the North American Society of Pacing and Electrophysiology, 1996) suggest a number of simple time domain measures to estimation HRV. It has been discussed in their paper that the HRV is calculated using the mean the standard deviation of the length of the cardiac cycle. This can be determined using either the R-R intervals of a short ECG segment or the. *a-a* intervals With these methods either the heart rate or the *a-a* intervals a and SDPTG signal. Table 2 shows some simple time–domain HRV variables: MAX-MIN, SDNN, RMSSD, and SDSD that can be calculated based on SDPTG signals.

Table 2: HRV Statistical Variables.

variable	Statistical measurement
MAX-MIN	Difference between shortest and longest *a-a* interval
SDNN	Standard deviation of all *a-a* intervals
RMSSD	Root mean square of the difference of successive *a-a* intervals
SDSD	Standard deviation of of differences between adjacent *a-a* intervals

5 CONCLUSIONS

The second derivative of the photoplethysmogram (SDPTG) can be used to calculate heart rate variability provided the *a*-waves can be detected accurately. Therefore, we propose an algorithm to detect *a*-waves in SDPTG signals with a high frequency noise, low amplitude, non-stationary effects, irregular heart beat and after exercise. It achieved an overall average sensitivity for *a*-waves detection 100% and a positive predictivity was 99.88%. over 27 records, containing a total of 3370 heart beats.

The accurate detection of *a*-waves in the SDPTG offers a non-invasive method of evaluating cardiac functioning. The usage of SDPTG can be useful for HRV analysis and identification of individuals at risk.

ACKNOWLEDGEMENTS

The authors would like to thank Aya Matsuyama for collecting the data.

REFERENCES

Berntson, G., Jr Bigger, J., Eckberg, D., Grossman, P., Kaufmann, P., Malik, M., Nagaraja, H., Porges, S.,

Saul, J., Stone, P. & Van Der Molen, M. (1997) Heart Rate Variability: Origins, Methods, And Interpretive Caveats. *Psychophysiology. ,* 34**,** 623-48.

Giardino, N., Lehrer, P. & Edelberg, R. (2002) Comparison Of Finger Plethysmograph To Ecg In The Measurement Of Heart Rate Variability. *Psychophysiology,* 39**,** 246-253.

John, D., & Catherine, T. Macarthur Research Network On Socioeconomic Status And Health. (2000) Heart Rate Variability.

Takazawa, K., Fujita, M., Kiyoshi, Y., Sakai, T., Kobayashi, T., Maeda, K., Yamashita, Y., Hase, M. & Ibukiyama, C. (1993) Clinical Usefulness Of The Second Derivative Of A Plethysmogram (Acceralation Plethysmogram). *Cardiology***,** 23:207-217.

Taniguchi, K., Nishikawa, A., Nakagoe, H., Sugino, T., Sekimoto, M., Okada, K., Takiguchi, S., Monden, M. & Miyazaki, F. (2007) Evaluating The Surgeon's Stress When Using Surgical Assistant Robots. *Robot And Human Interactive Communication, 2007. Ro-Man 2007. The 16th Ieee International Symposium On***,** 888-893.

Task Force Of The European Society Of Cardiology And The North American Society Of Pacing And Electrophysiology (1996) Heart Rate Variability: Standards Of Measurement, Physiological Interpretation, And Clinical Use. *Circulation,* 93**,** 1043-1065.